



HAL
open science

Fighting against medicine packaging counterfeits: rotogravure press vs cylinder signatures

Iuliia Tkachenko, Alain Tremeau, Thierry Fournel

► **To cite this version:**

Iuliia Tkachenko, Alain Tremeau, Thierry Fournel. Fighting against medicine packaging counterfeits: rotogravure press vs cylinder signatures. 2020 IEEE International Workshop on Information Forensics and Security (WIFS), Dec 2020, New York (virtual), United States. pp.1-6, 10.1109/WIFS49906.2020.9360883 . hal-03154680

HAL Id: hal-03154680

<https://hal.science/hal-03154680v1>

Submitted on 1 Mar 2021

HAL is a multi-disciplinary open access archive for the deposit and dissemination of scientific research documents, whether they are published or not. The documents may come from teaching and research institutions in France or abroad, or from public or private research centers.

L'archive ouverte pluridisciplinaire **HAL**, est destinée au dépôt et à la diffusion de documents scientifiques de niveau recherche, publiés ou non, émanant des établissements d'enseignement et de recherche français ou étrangers, des laboratoires publics ou privés.

Fighting against medicine packaging counterfeits: rotogravure press vs cylinder signatures

Iuliia Tkachenko
LIRIS

UMR CNRS 5205, Université Lumière Lyon 2
5 av. P. Mendès-France, 69676 Bron, France
Email: iuliia.tkachenko@univ-lyon2.fr

Alain Trémeau, Thierry Fournel
Laboratoire Hubert Curien

UMR CNRS 5516, Université de Lyon, UJM-Saint-Etienne
18 rue Pr. B. Lauras, 42000 Saint-Etienne, France
Email: {alain.tremeau, thierry.fournel}@univ-st-etienne.fr

Abstract—The number of medicine counterfeits increases significantly. This problem affects not only expensive medicines, but also some low cost ones. In this paper, we study the characteristics of medicine packages printed using rotogravure printing on blister foils and propose an authentication system that identifies the equipment used for printing medicine foils. The rotogravure printing process uses an engraved cylinder and a rotogravure press. Each of these elements has its own signature that can be used for process identification and for packaging authentication. Using constructed database, we show that the signature of engraved cylinder impacts more on printed patterns in comparison with the signature of rotogravure press. The experiments done show that we can identify the cylinder used for the printing using a classical machine learning methods from a small number of training samples.

I. INTRODUCTION

Product counterfeiting is one of the biggest problem nowadays. The actual pandemic situation is a paradise for medicine’s counterfeiters. The European Anti-Fraud Office reported identification of more than 340 companies trading in counterfeit products¹. Medicines market is one of the most sensitive markets as the counterfeits affect the human health and can cause the damage of brand reputation. The medicine protection can be based on some security elements that are inserted to the pharmaceutical packaging. In this way, the most common elements make use of some specific means as special inks and sticky labels [1], or consist in some optical variable device as the so-called holograms. They are a target for counterfeiters. International regulation and the cost security features represent for pharmaceutical companies enforces this as the graphical design complexity is sometimes minimal [2]. Adding feature elements is not really in adequacy with the protection of cheap medicines packaging. Alternatively, the use of intrinsic texture features of the packaging material and smart devices [3], [4] can provide a cheap, convenient protection. The system presented in [4], [5] suggests the use of a mobile device in a machine learning approach with pre-defined database to identify the manufacturer

¹Inquiry into fake COVID-19 products progresses https://ec.europa.eu/anti-fraud/media-corner/news/13-05-2020/inquiry-fake-covid-19-products-progresses_en

and the product using some physical textures that are found in blister and carton packaging of medicines. In practice, intrinsic features extraction is part of a protocol devoted to securing goods data [6].

Printing some black-and-white copy sensitive graphical codes [7], [8] is another approach, well-suited to a remote verification of packaging with smart readers, such an approach remaining low cost. A theoretical comparison with the intrinsic approach based on hypothesis testing can be found in [9]. Experimentally, the existing implementations were nevertheless only tested with office paper or carton, and laser printers.

On the other hand, the blister packaging is the most used support for medicines. In order to print on blister foils one has to use specific printing devices. One of the commonly used printing processes is rotogravure printing [10] which is significantly different in comparison with inkjet and laser printing. Taking into account the specific conditions of production process of medicine packaging, it will be good to find a solution that is similar to image forensics or printer/scanner forensics [11], [12], [13], and that could be easily controlled by authorities, pharmacists and customers.

The rotogravure printing has several particularities and specific characteristics as serrated edges, missing dots and “doughnuts” [14]. The packaging artwork has first to be engraved in a cylinder using a suitable process among chemical, electrochemical or laser processes. Then, the engraved cylinder is used in a press system able to print on metallic foils more than one million of packaging per cylinder. In this paper our aim is to study the printing process on medicine blister foils when using chemical engraving process for cylinders, and use its variability for rotogravure press and cylinder identification. As text usually takes the biggest part of medicine blister packaging, for the identification we operate directly on printed text characters, without any special print or requirement.

As far as we know this is the first paper that study the character forensics of rotogravure printing packages. We show in this paper that: 1) each engraved cylinder has its own signature due to the stochastic nature of engraving process; 2) the signature of engraving process impacts more the printed packaging than the press signature; 3) both signatures can be used for cylinder identification and thus detection of counterfeits.

To validate our hypothesis: firstly we characterized the ro-

togravure printing and create the first database of text characters printed by a rotogravure press on blister foils²; next we studied the impact of cylinder and printer signatures; lastly we constructed the control system that can correctly perform rotogravure press and cylinder identification in possible counterfeiting situations.

The rest of the paper is organized as follows. We quickly introduce the rotogravure process in Section II. The proposed authentication system, as well as the method used for cylinder identification, are presented in Section III. The experimental results are discussed in Section IV. Finally, we conclude and present some future paths in Section V.

II. ROTOGRAVURE PRINTING

Rotogravure printing is often used for production of magazines, catalogs and packaging (from extremely thin foils to thick cardboard) thanks to rapid printing process, production of high-quality images and intense rich colors. Each primary color is printed using a cylinder that is passed to the press. Each cylinder with specific color composes an ink unit.

The printing process consists of three main steps: 1) design of artwork for each color unit; 2) cylinder engraving according to the designed artwork; 3) printing using the engraved cylinder/s. The artwork is usually created using some design software (like CorelDraw or PhotoShop). The designed artwork is then pre-processed in order to define the main printing parameters of the engraving process. In this stage, the engineers: 1) define what width of lines will be used; 2) correct the edges, manage the overlaps and minimize the color border imperfections using trapping process; 3) define the number of colors used and the order of cylinders used for printing process; 4) define the screen angles depending on printing support used; 5) define the dots shape (elongated, compressed or normal); 6) define the cell depth. After all these pre-processing steps, the artwork is ready to be engraved on the cylinder.

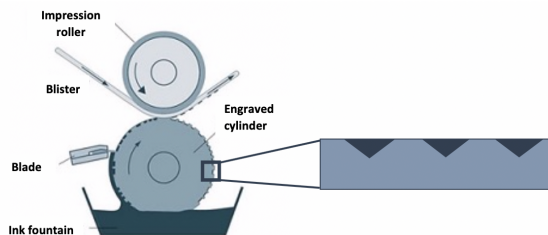


Fig. 1. The printing process using rotogravure. Cylinder cells shown are a graphical illustration of electronic/mechanical engraving

Cylinder can be engraved using 3 different technologies: chemically, electro-mechanically and by laser. Depending on the engraving process, the form of dots and the quality of printed edges is different. In this paper, we use samples printed using chemically engraved cylinders. Chemical etching

is the oldest method for cylinder engraving. With this process, all engraved cells have the same size, and the thickness of the membrane between cells remains constant. In practice, chemical engraving has some variability at a micro-scale.

To print each color, we need one engraved cylinder, thus the rotogravure printing consists of several color units. The general scheme of one color unit is illustrated in Fig. 1. It consists of the engraved cylinder, the press and an ink pan. The engraved cylinder rotates through an ink pan. The image areas correspond to the cells that pick the ink from this ink pan. The non-image areas and the over quantity of ink are scarped by a blade before the ink is transferred to a support (paper or blister) surface. After each color unit, the ink is dried using high velocity air nozzle dryer.

Rotogravure printing can usually produce richer colors than other printing processes, thanks to the ability of this process to lay down a thick three-dimensional ink film - altering not only the width of the dots but also the depth [15]. Nevertheless, a typical characteristic of rotogravure is its serrated edges on type and line work [15]. In addition, the rotogravure method is sensitive to surface defects (blade lines and indentations). During rotogravure printing, the ink is pulled out of cells. The most common shape of cells is an inverted pyramid. If the bottom of the cell does not release the ink quickly, it results in non-uniform ink coverage. As the result, a rotogravure printing is characterized often either by missing dots (result of ink transfer failure) or by dots with holes in their center or on a board (that called "doughnuts"). Some examples of these characteristics were presented in [14].

III. SUGGESTED AUTHENTICATION SYSTEM

Let W be an artwork, a digital image with several replications of a given pharmaceutical packaging serving as input to the (chemical) process for cylinder manufacturing. Let e_i be the letter 'e' located in position i in artwork W (some other frequent letters composed with straight and curved lines as 'a' could be also used). Fig. 2 shows a scheme where both the artwork and cylinder engraved with letters e_i are represented. In the following, we will investigate the signature of engraving and press in such letters.

A. Cylinder vs Press signature

In [14], it was spotted that the engraved cylinder of a specific rotogravure printing system transmits its own spatial "signature" that can be measured by image correlation. It has been shown the uniqueness of text characters printed using rotogravure process.

However, as rotogravure printing process consists of engraving process and printing process, we do not know which process impacts more to the signature. In this paper, we assume that all text characters printed with the same engraved part of the cylinder have higher correlation values than the text characters printed using another engraved part. We will validate experimentally this assumption in Section IV.

On the other hand, as with laser and inkjet printers [11], [13], each printed character contains the press signature. The only

²The database is available on demand. Contact: iuliiia.tkachenko@univ-lyon2.fr

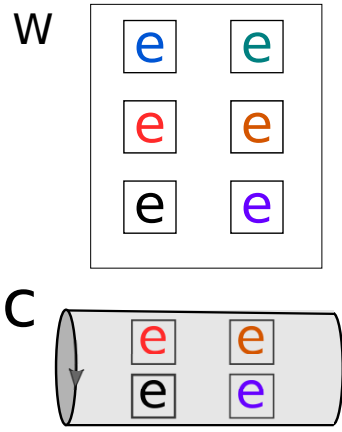


Fig. 2. Graphical representation of an artwork and the corresponding engraved letters on a rotogravure cylinder.

thing one need to study is the impact of each signature. That means we need to test: either the text characters differ more from one rotogravure press to another rotogravure press (in this case, we must fix the cylinder and change the press used); or the text characters differ more from one cylinder to another cylinder (in this case, we must fix the press and use some cylinders engraved using the same method).

Cylinder	Press
Fixed	Variable
Variable	Fixed
Variable	Variable

TABLE I

DIFFERENT COMBINATIONS OF CYLINDER AND PRESS IN ORDER TO UNDERSTAND WHOSE SIGNATURE IS MORE IMPORTANT DURING AUTHENTICATION.

In order to understand which signature is more important, we need to analyze different combinations of press and cylinder as described in Table I. All these situations are possible both in the authentic scenario (when we have a lot of authentic presses and cylinders to print a big amount of authentic packages) and in the counterfeited scenario (an opponent can either have an access to the authentic rotogravure press or cylinders or can produce new cylinders and print using new press). Nevertheless, the most realistic situation for an attack is the situation when an opponent does not have access to the authentic cylinders and rotogravure press, thus s/he needs to produce its own cylinders and to print the counterfeited packages using his own press.

B. Authentication system based on cylinder signature

As for counterfeiting, any opponent needs to produce a new engraved cylinder, the cylinder forensic investigation is a good path for detection of counterfeits. Let $I_a = \Pi_a(E_a(W))$ be an authentic artwork image after cylinder engraving and printing, where E_a is a noise added by the engraving process and Π_a is a noise added by the rotogravure printing. We suppose that all images I_a , printed using an authentic cylinder E_a and an authentic rotogravure press Π_a , have some specific

characteristics due to cylinder and press signatures. Thus, all these images belong to the class C_a ($\forall I_a \in C_a$).

On the other hand, even if the counterfeiter can predict exactly the same digital artwork W (in the case of medicine packaging that contains of text only, it is quite easy) and produce a counterfeited cylinder E_c , the images printed using this cylinder will be different $I_c = \Pi_c(E_c(W)) \in C_c$ due to the signature of the counterfeited cylinder E_c and of the other rotogravure press Π_c used.

Consequently, the authentication test can be formulated as a hypothesis test:

$$H_0 : I' \in C_a,$$

$$H_1 : I' \notin C_a,$$

where I' is a new captured image of the printed artwork. The image I' can be considered as authentic when H_0 hypothesis is accepted, otherwise I' cannot be considered as authentic.

C. Authentication system overview

In this paper, we suggest to extract the most relevant image features using PCA (Principal Component Analysis) and to compare the distances between the images in the train database and test database.

The train database consists of n images. Thanks to the PCA, each image $T_i, i = 1, \dots, n$ from the train database is represented as a linear combination of all eigenvectors:

$$T_i = \Psi + \omega_1 \cdot U_1 + \dots + \omega_n \cdot U_n,$$

where Ψ is the average image, $\Omega_i = [\omega_1, \dots, \omega_n]$ is a weight vector for image T_i and $U_j, j = 1, \dots, n$ is the eigenvector j in matrix representation.

During the testing stage, each image I' is projected onto the eigenspace and the corresponding weight vector Ω' is computed. In order to detect the class of images (authentic cylinder and press used or counterfeiter cylinder and press used) which best corresponds to this image, we calculate the distance between the input weight vector Ω' and all weight vectors of the training set $\Omega_i, i = 1, \dots, n$. The minimal distance indicates the class of image I' which best corresponds to this image.

As it was mentioned in the previous section, the images that were printed using the same press and the same cylinder should belong to the same class. In the case of realistic attack, when an attacker uses a new cylinder and a new rotogravure press, any image from this class must be rejected as an anomaly by our authentication system. For this purpose, we suggest to use a threshold Th that can be empirically defined during the validation step. Therefore, when the smallest distance between a test image weight vector Ω' and all weight vectors of the training set $\Omega_i, i = 1, \dots, n$ is bigger than a threshold Th , the image I' is rejected as a suspicious packaging.

IV. EXPERIMENTAL RESULTS

A. Database description

In our experiments, we used cylinders engraved using the chemical process. This engraving process is the cheapest one and is currently the most used for medicine packaging production. The text samples used were printed on aluminum blisters using black ink.

We created a database using two rotogravure presses of the same brand (P_1 and P_2) and two similarly engraved cylinders (C_1 and C_2). The screen ruling of the cylinder was 70 lines per cm (or 178 lines per inch). The same blister foil and liquid ink (foil ink) were used for production of these printed samples. We used the letters 'e' as it is the most used letter in English language. The database contains gray-scale images of 359×418 pixels size. All images were captured using USB-microscope with $\times 5$ magnification. Several samples from this database are illustrated in Fig. 3. We can notice that each rotogravure press and each cylinder produce the same letter but with specific signature.

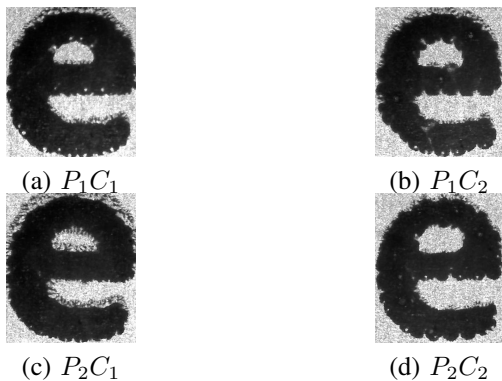


Fig. 3. Illustration of cylinder signature while engraving the same artwork four times on the same cylinder: a) letter 'e' engraved on cylinder C_1 and printed using press P_1 , b) letter 'e' engraved on cylinder C_2 and printed using press P_1 , c) letter 'e' engraved on cylinder C_1 and printed using press P_2 , d) letter 'e' engraved on cylinder C_2 and printed using press P_2 .

The database, created specifically for this study, contains 450 samples from each chemically engraved cylinder and rotogravure press. These samples come from 25 aluminum foil pages (one page corresponds to one turn of cylinder). Each page contains 18 positions of the letter 'e'. The database details are given in Table II.

	Nb of positions	Nb of pages	Total number
P_1C_1	18	25	450
P_2C_1	18	25	450
P_1C_2	18	25	450
P_2C_2	18	25	450

TABLE II

DIFFERENT COMBINATIONS OF CYLINDER AND PRINTER USED FOR TESTS.

B. Impact of signatures

In order to study the impact of rotogravure press and cylinder signatures, we studied the following scenarios (as described in Table I):

- images printed using variable presses and the same cylinder (P_1C_1 vs P_2C_1);
- images printed using the same press and variable cylinders (P_1C_1 vs P_1C_2);
- images printed using variable presses and cylinders (P_1C_1 vs P_2C_2).

In order to analyze the impact of these three situations, we used the t-SNE method (T-distributed Stochastic Neighbor Embedding) [16]. This 2D visualization method enables to show the impact of each signature thanks to the good or bad separation of data in clusters.

In the first experiment we did, we fixed the engraved cylinder (C_1) and used two rotogravure presses (P_1 and P_2) for printing the samples. The results are illustrated in Fig. 4. We can notice that we do not have separated clusters. Thus, the signature of rotogravure press does not impact a lot the printing quality of letters 'e'. Consequently, it seems quite challenging to identify the text characters printed using the same cylinder and two different rotogravure presses.

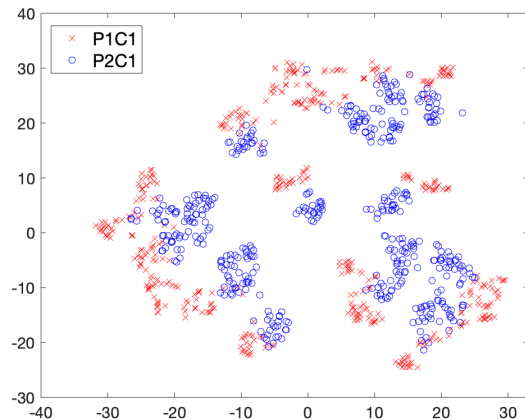


Fig. 4. Investigation of printer signature. Comparison of samples that were printed using the same engraved cylinder (C_1) and two rotogravure presses (P_1 and P_2).

In the second experiment, we fixed the rotogravure press (P_1) and used two engraved cylinders (C_1 and C_2) for printing the samples. The results are illustrated in Fig. 5. We can notice that now the clusters are well separated, but this separation is not linear.

In the third experiment, we used two presses (P_1 and P_2) and two engraved cylinders (C_1 and C_2) for printing the samples. This experiment corresponds to the case of real attack, when an authority center uses the press P_1 and the authentic cylinder C_1 , meanwhile an attacker uses a press P_2 and a counterfeited cylinder C_2 . The results are illustrated in Fig. 6. These results show that the signature of printer and cylinder together enable to get a good separation between the authentic and counterfeited samples.

The results of these experiments demonstrate that the signature of the engraving process impacts more the image quality than

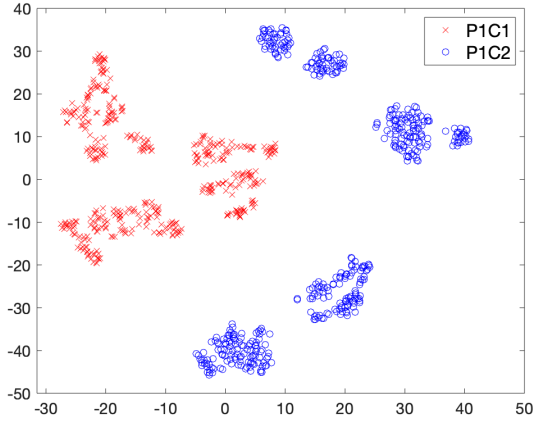


Fig. 5. Investigation of cylinder signature. Comparison of samples that were printed using two engraved cylinders (C_1 and C_2) and one press (P_1).

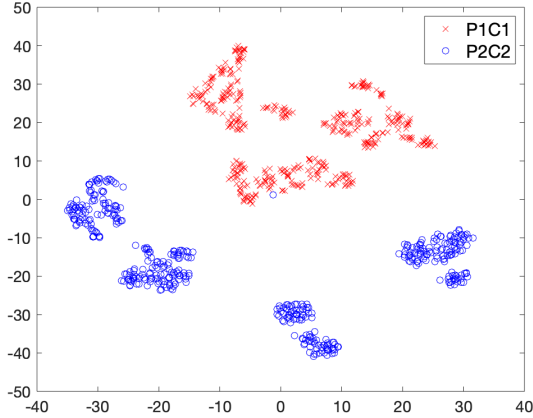


Fig. 6. Investigation of cylinder and press signature. Comparison of samples that were printed using press P_1 with cylinder C_1 and using press P_2 with cylinder C_2 .

the signature of the printing process and can be efficiently used for cylinder identification and packaging authentication.

C. Cylinder identification

The classification of text characters 'e' was performed using the minimal distance between the weights vectors obtained using the PCA. The results are presented in Table III. As expected, the accuracy is improved when the train database contains more samples. Intentionally, we use a small number of samples for the train database, as it is very challenging to create big databases in real industrial setups.

In order to compare the obtained results with another classifier, we decided to use the NNLS (Non-Negative Least Squares) sparse coding classifier [17], [18]. We used the Sparse Representation Toolbox in MATLAB version 1.9 that is publicly available³. The classification results are presented in Table IV.

³Sparse Representation Toolbox in MATLAB version 1.9 <https://sites.google.com/site/sparserep-tool/>

	Predicted classes			
	P_1C_1	P_2C_1	P_1C_2	P_2C_2
1 image per class				
P_1C_1	51.93%	7.73%	29.23%	11.11%
P_2C_1	47.58%	45.17%	6.52%	0.72%
P_1C_2	0.00%	0.00%	47.10%	52.90%
P_2C_2	0.00%	0.00%	48.55%	51.45%
9 images per class				
P_1C_1	64.49%	32.85%	1.21%	1.45%
P_2C_1	24.15%	75.36%	0.00%	0.48%
P_1C_2	0.00%	0.00%	33.82%	66.18%
P_2C_2	0.00%	0.00%	35.75%	64.25%
18 images per class				
P_1C_1	62.32%	35.75%	1.21%	0.72%
P_2C_1	5.07%	94.44%	0.00%	0.48%
P_1C_2	0.00%	0.00%	29.47%	70.53%
P_2C_2	0.00%	0.00%	28.99%	71.01%
36 images per class				
P_1C_1	73.43%	24.88%	0.97%	0.72%
P_2C_1	6.28%	93.48%	0.00%	0.24%
P_1C_2	0.00%	0.00%	47.58%	52.42%
P_2C_2	0.00%	0.00%	46.62%	53.38%

TABLE III

RESULTS OF THE PCA CLASSIFICATION WITH DIFFERENT NUMBERS OF IMAGES PER CLASS IN THE TRAINING SET.

	Predicted classes			
	P_1C_1	P_2C_1	P_1C_2	P_2C_2
9 images per class				
P_1C_1	71.53%	23.15%	3.01%	2.31%
P_2C_1	2.95%	96.83%	0.00%	0.23%
P_1C_2	0.00%	0.00%	19.91%	80.09%
P_2C_2	0.00%	0.00%	16.20%	83.80%
18 images per class				
P_1C_1	77.05%	17.63%	4.35%	0.97%
P_2C_1	2.36%	97.40%	0.00%	0.24%
P_1C_2	0.00%	0.00%	36.47%	63.53%
P_2C_2	0.00%	0.00%	30.68%	69.32%

TABLE IV

RESULTS OF THE NNLS CLASSIFICATION WITH DIFFERENT NUMBERS OF IMAGES PER CLASS IN THE TRAINING SET.

We can see that the results are quite similar to the results obtained with the PCA. Both classifiers can efficiently separate the images that were obtained using a specific cylinder. Nevertheless, there are a lot of classification errors between images when these are printed by the same cylinder but different rotogravure presses. For example, there are a lot of misclassification between classes P_1C_2 and P_2C_2 in Table III and Table IV. The experiments we did demonstrate the importance of the engraving process impact.

D. Packaging authentication

In this section, we compare the distances between the weights vectors obtained with the PCA and a threshold for image rejection (i.e. identification of images that were printed using unknown cylinder and rotogravure press).

The train database consists of 18 (36) samples printed using cylinder C_1 and press P_1 . First, we determined the weight vectors of the training set $\Omega_i, i = 1, \dots, 18(36)$. Next, we used a validation set of 54 samples printed using cylinder C_1 and press P_1 in order to determine the threshold Th , that will be used for rejection of images that have minimal distance

bigger than this threshold. The value of this threshold was calculated such as:

- $Th_1 = \text{mean}(dist_{valid})$ is the mean value of the 54 minimal distances of the validation set;
- $Th_2 = \text{mean}(dist_{valid}) - \text{mean}(dist_{valid}) \times 0.5$;
- $Th_3 = \text{mean}(dist_{valid}) - \text{mean}(dist_{valid}) \times 0.7$;
- $Th_4 = \text{max}(dist_{valid})$ is the maximal value of the 54 minimal distances of the validation set.

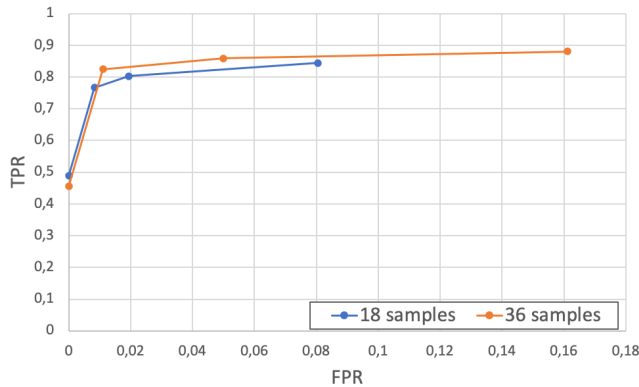


Fig. 7. ROC curve that represents the classification results depending on the selected threshold.

The test database consists of 360 samples that were printed using cylinder C_1 and press P_1 , and 360 samples that were printed using cylinder C_2 and press P_2 . The ROC curve of the classification results obtained is illustrated in Fig. 7. We can notice that the best trade-off between the number of true positive (TPR) and false positive rates (FPR) is obtained using the Th_2 , while using 36 samples in the train database. Even if we have more than 10% of rejection of authentic samples, we have also more than 95% of counterfeited samples that were rejected using such a small training database. Certainly, these results could be significantly improved using a bigger training database.

V. CONCLUSIONS

In this paper, we investigated the authentication of medicine packaging printed using rotogravure process. We studied the impact of a printing process using a chemically engraved cylinder and a rotogravure press. Based on the obtained results and of the chemical nature of the engraving process, we can conclude that the engraving process (using chemical etching) can be considered as a stochastic process. We showed that, even if an opponent can correctly estimate the artwork used (or even has access to the original artwork), the replication of the exact shape of a printed text character at a micro-scale with similar means is not feasible in practice. Therefore, passing the proposed authentication test is rather unlikely.

Using the impact of the engraving process we can not only identify the cylinder that was used for medicine packaging production, but can also detect counterfeited blisters. The experimental results showed that we can use a small number of training images and a classical classifier, based on the Principal

Component Analysis or the Non-negative Least Squares, to authenticate medicine packaging.

In future we would like to exploit the position of each character in the engraved cylinder in order to improve the classification results. In addition, we would like to employ advanced machine learning methods as few-shot learning to improve the accuracy and robustness of the classification.

ACKNOWLEDGEMENTS

This work was funded by project *PackMark* supported by the Indo-French Center for the Promotion of Advanced Research (IFCPAR) under contract IFCPAR-7127.

REFERENCES

- [1] R. L. Van Renesse, *Optical document security. Third edition.* Artech House optoelectronics library, 2005.
- [2] M. Davison, *Pharmaceutical anti-counterfeiting: combating the real danger from fake drugs.* John Wiley & Sons, 2011.
- [3] C.-W. Wong and M. Wu, "Counterfeit detection based on unclonable feature of paper using mobile camera," *IEEE Transactions on Information Forensics and Security*, vol. 12, no. 8, pp. 1885–1899, 2017.
- [4] R. Schraml, L. Debiase, C. Kauba, and A. Uhl, "On the feasibility of classification-based product package authentication," in *2017 IEEE Workshop on Information Forensics and Security (WIFS)*. IEEE, 2017, pp. 1–6.
- [5] R. Schraml, L. Debiase, and A. Uhl, "Real or fake: Mobile device drug packaging authentication," in *Proceedings of the 6th ACM Workshop on Information Hiding and Multimedia Security*, 2018, pp. 121–126.
- [6] T. Fournel, J. Becker, and Y. Boutant, "Self-encryption for paper document authentication," in *Journal of Physics: Conference Series*, vol. 77, no. 1, 2007, pp. 7–12.
- [7] J. Picard, Z. Sagan, A. Foucou, and J.-P. Massicot, "Method and device for authenticating geometrical codes," May 20 2014, uS Patent 8,727,222.
- [8] I. Tkachenko, W. Puech, C. Destruel, O. Strauss, J.-M. Gaudin, and C. Guichard, "Two-level QR code for private message sharing and document authentication," *IEEE Transactions on Information Forensics and Security*, vol. 11, no. 3, pp. 571–583, 2016.
- [9] S. Voloshynovskiy, T. Holotyak, and P. Bas, "Physical object authentication: detection-theoretic comparison of natural and artificial randomness," in *2016 IEEE International Conference on Acoustics, Speech and Signal Processing (ICASSP)*. IEEE, 2016, pp. 2029–2033.
- [10] H. Kipphan, *Handbook of print media: technologies and production methods.* Springer Science & Business Media, 2001.
- [11] A. K. Mikkilineni, N. Khanna, and E. J. Delp, "Forensic printer detection using intrinsic signatures," in *Media Watermarking, Security, and Forensics III*, vol. 7880. International Society for Optics and Photonics, 2011, p. 78800R.
- [12] N. Khanna and E. J. Delp, "Source scanner identification for scanned documents," in *Information Forensics and Security, 2009. WIFS 2009. First IEEE International Workshop on*. IEEE, 2009, pp. 166–170.
- [13] L. C. Navarro, A. K. Navarro, A. Rocha, and R. Dahab, "Connecting the dots: Toward accountable machine-learning printer attribution methods," *Journal of Visual Communication and Image Representation*, vol. 53, pp. 257–272, 2018.
- [14] I. Tkachenko, A. Trémeau, and T. Fournel, "Authentication of medicine blister foils: Characterization of the rotogravure printing process," in *Proceedings of the 14th International Joint Conference on Computer Vision, Imaging and Computer Graphics Theory and Applications - Volume 4: VISAPP, INSTICC*. SciTePress, 2019, pp. 577–583.
- [15] M. G. Keif and T. Goglio, "Identifying high-volume printing processes," *Visual Communications Journal*, p. 35, 2005.
- [16] L. v. d. Maaten and G. Hinton, "Visualizing data using t-sne," *Journal of machine learning research*, vol. 9, no. Nov, pp. 2579–2605, 2008.
- [17] Y. Li and A. Ngom, "Nonnegative least-squares methods for the classification of high-dimensional biological data," *IEEE/ACM transactions on computational biology and bioinformatics*, vol. 10, no. 2, pp. 447–456, 2013.
- [18] —, "Classification approach based on non-negative least squares," *Neurocomputing*, vol. 118, pp. 41–57, 2013.